

Gd-complexes of DTPA-bis(amide) conjugates of tranexamic acid and its esters with high relaxivity and stability for magnetic resonance imaging

Sujit Dutta,^a Ji-Ae Park,^b Jae-Chang Jung,^c Yongmin Chang^{*b,d,e} and Tae-Jeong Kim^{*a}

Received 18th December 2007, Accepted 25th February 2008

First published as an Advance Article on the web 13th March 2008

DOI: 10.1039/b719440d

The synthesis and the characterization of a series of DTPA-bis(amide) conjugates of tranexamic acid (**L1**), its esters (**L2–L6**), and their Gd(III) complexes of the type $[\text{Gd}(\text{L})(\text{H}_2\text{O})] \cdot n\text{H}_2\text{O}$ (**L** = **L1–L6**) are described. Except for the case of **L1**, all Gd-complexes exhibit greatly enhanced R_1 relaxivity. Highest R_1 reaches up to $12.9 \text{ mM}^{-1} \text{ s}^{-1}$ for $[\text{Gd}(\text{L2})(\text{H}_2\text{O})]$. Such high relaxivity is reflected in the intensity enhancement of the *in vivo* MRI study on H-ras transgenic mice bearing hepatic tumor when employing $[\text{Gd}(\text{L2})(\text{H}_2\text{O})]$ as an MRI contrast agent. Thermodynamic stability constants, conditional stability constants, and the pM values demonstrate higher stability of $[\text{Gd}(\text{L})(\text{H}_2\text{O})] \cdot n\text{H}_2\text{O}$ (**L** = **L1–L6**) than Omniscan[®] under physiological conditions. The MTT assay performed on these complexes reveals cytotoxicity as low as that for Omniscan[®] in the concentration range required to obtain intensity enhancement in the *in vivo* MRI study.

Introduction

Magnetic resonance imaging (MRI) provides high-resolution three-dimensional images of the internal part of the body depending on the difference in the *in vivo* distribution of the water molecules. Noninvasive nature and excellent spatial resolution at the sub-millimeter level render MRI as a powerful diagnostic imaging modality. The relatively low sensitivity of MRI can be overcome by inducing additional contrast in the MR images by the introduction of a contrast agent (CA) prior to the MRI test.¹ These contrast agents catalytically shorten the relaxation time of the nearby water molecules to enhance the contrast with the background tissues in the MR images. The enhanced usage of MRI as the diagnostic imaging modality prompts the development of efficient MRI CAs.² The Gd(III) ion is known to possess the highest paramagnetism of all metal ions and Gd(III) complexes incorporating macrocyclic or acyclic poly(aminocarboxylate) ligands have so far been used widely as MRI CAs. The Gd-based MRI CAs currently available for clinical uses may be classified into two types: (1) an anionic type such as bis-*N*-methylglucamine salt of $[\text{Gd}(\text{DTPA})(\text{H}_2\text{O})]^{2-}$ (DTPA = diethylenetriamine-*N,N,N',N'',N'''*-pentaacetic acid) (Magnevist[®]); (2) a neutral type such as $[\text{Gd}(\text{DTPA-BMA})(\text{H}_2\text{O})]$ (DTPA-BMA = *N,N''*-bis(methylamide) of DTPA) (Omniscan[®]) and $[\text{Gd}(\text{HP-DO3A})(\text{H}_2\text{O})]$ (HP-DO3A = 20-(2-hydroxypropyl) derivative of 1,4,7,10-tetraazacyclododecane-*N,N',N'',N'''*-1,4,7-tetraacetic acid) (Prohance[®]). Of

the two types, the latter is preferred because of relatively low osmotic pressure in the body fluids after intravenous administration.^{3,4} Yet, a great number of neutral Gd-complexes incorporating DTPA-bis(amide) ligands are known and some of them are known to exhibit poor water solubility.^{5–12} It is worth noting that high relaxivity and non-cytotoxicity in addition to high water solubility are the essential criteria for an efficient MRI CA.

We have recently demonstrated that a slight modification of the ligand such as introduction of polar groups to the alkyl substituents on the amide N-atoms of DTPA-bis(amide) can lead to the formation of a series of highly water-soluble Gd-complexes. To our disappointment, however, their use as MRI CAs has been frustrating due to poor relaxivity.¹³ In an effort to overcome this problem and at the same time meet the three-fold requirement for an effective MRI CA mentioned above, we have developed a new strategy to further modify DTPA-bis(amide): introduction of polar alkyl substituents with high molecular weight on the amide N-atoms in such a way that the polar groups are directed as far away from the Gd(III) center as possible to minimize any interference with the water exchange equilibrium between the coordinated and the bulk water molecules. Suitable candidates for the substituents to meet the above criteria may include *trans*-4-(aminomethyl)-cyclohexanecarboxylic acid (tranexamic acid) and the corresponding esters. Further rationalization for their selection may come from the fact that tranexamic acid and its derivatives have been used as antifibrinolytic drugs with no sign of cytotoxicity.^{14–16}

Herein, we report the syntheses of DTPA-bis(amide) conjugates of tranexamic acid (**L1**) and its esters (**L2–L6**) and their Gd(III) complexes, $[\text{Gd}(\text{L})(\text{H}_2\text{O})] \cdot n\text{H}_2\text{O}$ (**L** = **L1–L6**). Also reported are the studies relevant to the potential application of these complexes as practical MRI CAs.

Experimental

General remarks

All reactions were carried out under an atmosphere of dinitrogen using the standard Schlenk techniques. Solvents were purified

^aDepartment of Applied Chemistry, Kyungpook National University, Daegu, 702-701, Korea. E-mail: tjkim@knu.ac.kr; Fax: +82-53-950-6594; Tel: +82-53-950-5587

^bDepartment of Medical & Biological Engineering, Kyungpook National University, Daegu, 702-701, Korea. E-mail: ychang@knu.ac.kr; Fax: +82-53-422-2677; Tel: +82-53-420-5471

^cDepartment of Biology, Kyungpook National University, Daegu, Korea 702-701

^dDepartment of Diagnostic Radiology, Kyungpook National University, Daegu, Korea 702-701

^eDepartment of Molecular Medicine, Kyungpook National University, Daegu, Korea 702-701

and dried using standard procedures. Diethylenetriamine-*N,N,N',N'',N''*-pentaacetic acid (DTPA) and *trans*-4-(aminomethyl)cyclohexanecarboxylic acid were obtained from TCI and used without further purification. The *N,N*-bis(anhydride) of DTPA,¹⁷ methyl *trans*-4-(aminomethyl)cyclohexylcarboxylate,¹⁸ ethyl *trans*-4-(aminomethyl)cyclohexylcarboxylate,¹⁸ **L1**,¹⁸ **L2**,¹⁸ **L3**,¹⁸ [Gd(**L1**)H₂O],¹⁸ [Gd(**L2**)H₂O],¹⁸ and [Gd(**L3**)H₂O]¹⁸ were prepared according to the literature methods. All other commercial reagents were purchased from Aldrich and used as received unless otherwise stated. Deionized water was used for all experiments. The ¹H and ¹³C NMR experiments were performed on a Bruker Advance 400 or 500 Spectrometer by Korea Basic Science Institute (KBSI). Chemical shifts were given as δ values with reference to tetramethylsilane (TMS) as an internal standard. Coupling constants are in Hz. FAB-Mass spectra were obtained by using a JMS-700 model (Jeol, Japan) mass spectrophotometer. IR spectra were run on a Mattson FT-IR Galaxy 6030E spectrophotometer at KBSI. Elemental analyses were performed by Center for Instrumental Analysis, KNU.

Potentiometric measurements and computational method

Potentiometric titrations were performed with an automatic titrator to determine the protonation constants of the DTPA-bis(amide) ligands and the stability constants of corresponding metal complexes. The autotitrating system consists of a 798 MPT Titroprocessor, a 728 stirrer and a PT-100 combination pH electrode (Metrohm). The pH electrode was calibrated using standard buffer solutions. All calibrations and titrations were carried out under a CO₂-free nitrogen atmosphere in a sealed glass vessel (50 cm³) thermostatted at 25 \pm 0.1 °C at an ionic strength of 0.10 mol dm⁻³ KCl. The concentrations of the metal-ion and the amide solutions were maintained at approximately 0.6 mmol dm⁻³. A CO₂-free KOH solution (0.100 mol dm⁻³) was used as a titrant to minimize the changes in ionic strength during the titration. Dioxygen and carbon dioxide were excluded from the reaction mixtures by maintaining a positive pressure of purified nitrogen in the titration cell. The electromotive force of the cell is given by $E = E^\circ + Q \log[H^+] + E_j$, and both E° and Q were determined by titrating a solution with a known hydrogen-ion concentration at the same ionic strength, using the acid range of the titration. The liquid-junction potential (E_j) was found to be negligible under the experimental conditions employed. The protonation constants of the ligands and the overall stability constants of various metal complexes formed in aqueous solutions were determined from the titration data using the computer program HYPERQUAD.¹⁹ The accuracy of this method was verified by measuring the protonation and the stability constants for Ca(II), Zn(II), Cu(II) and Gd(III) complexes of [DTPA-BMA]³⁻. The results were compared with literature values.²⁰

Synthesis of the esters of *trans*-4-(aminomethyl)cyclohexylcarboxylic acid

2-Hydroxyethyl-*trans*-4-(aminomethyl)cyclohexylcarboxylate hydrochloride. To a stirred suspension of *trans*-4-(aminomethyl)cyclohexylcarboxylic acid (3.93 g, 25 mmol) in ethylene glycol (50 mL) cooled in a ice-bath was added thionyl chloride (3.57 g, 30 mmol) during 10 min. The reaction mixture was then heated at

75 °C for 1 h, after which the mixture was cooled to RT. The solvent was removed under a reduced pressure, and the residue triturated thrice with hexane (30 mL). The resulting solid was taken in methanol, treated with decolorizing charcoal, and the solvent removed under a reduced pressure. The resulting solid was dried *in vacuo* for 6 h. Yield 5.47 g (92%). ¹H NMR (*d*₆-DMSO, 400 MHz), δ 8.14 (br s, 3H, NH₂HCl), 4.27 (t, J = 5.02, 2H, OCH₂CH₂OH), 4.00 (t, J = 5.02, 2H, OCH₂CH₂OH), 2.61 (d, J = 7.04, 2H, H₉), 2.25 (m, 1H, H₁₃), 1.87 (m, 4H, H₁₁/H₁₂), 1.56 (m, 1H, H₁₀), 1.13 (m, 4H, H₁₁/H₁₂). ¹³C NMR (*d*₆-DMSO, 100 MHz), δ 175.29 (C1), 65.90 (OCH₂CH₂OH), 59.27 (OCH₂CH₂OH), 44.43 (CH₂NH₂), 42.39 (C2), 35.17 (C4), 29.02 (C3, C5), 28.20 (C2, C6). Anal. Calc. for C₁₀H₁₉NO₃HCl·0.5H₂O: C, 48.68; H, 8.58; N, 5.68. Found: C, 48.50; H, 8.37; N, 5.70%. FABMS (m/z): calc. for C₁₀H₂₀NO₃, 202.27 ([MH]⁺); found, 202.05.

2-Methoxyethyl-*trans*-4-(aminomethyl)cyclohexylcarboxylate hydrochloride. The title compound was prepared by the same procedure for 2-hydroxyethyl-*trans*-4-(aminomethyl)cyclohexylcarboxylate hydrochloride by replacing ethylene glycol with methoxyethanol. Yield 5.67 g (90%). ¹H NMR (*d*₆-DMSO, 400 MHz), δ 8.16 (br s, 3H, NH₂HCl), 4.11 (t, J = 4.52, 2H, OCH₂CH₂OCH₃), 3.50 (t, J = 4.52, 2H, OCH₂CH₂OCH₃), 3.25 (s, 3H, OCH₃), 2.61 (d, J = 6.88, 2H, H₉), 2.24 (m, 1H, H₁₃), 1.86 (m, 4H, H₁₁/H₁₂), 1.57 (m, 1H, H₁₀), 1.11 (m, 4H, H₁₁/H₁₂). ¹³C NMR (*d*₆-DMSO, 100 MHz), δ 173.79 (C1), 68.74 (OCH₂CH₂OCH₃), 61.89 (OCH₂CH₂OCH₃), 57.04 (OCH₃), 43.04 (CH₂NH₂), 40.93 (C2), 33.74 (C4), 27.63 (C3, C5), 26.81 (C2, C6). Anal. Calc. for C₁₁H₂₁NO₃HCl: C, 52.48; H, 8.81; N, 5.56. Found: C, 52.29; H, 8.67; N, 5.70%. FABMS (m/z): calc. for C₁₁H₂₂NO₃, 216.30 ([MH]⁺); found, 216.10.

Allyl-*trans*-4-(aminomethyl)cyclohexylcarboxylate hydrochloride. The title compound was prepared by following the same procedure as for 2-hydroxyethyl-*trans*-4-(aminomethyl)cyclohexylcarboxylate hydrochloride by replacing ethylene glycol with allyl alcohol. Yield 4.79 g (82%). ¹H NMR (*d*₆-DMSO, 400 MHz), δ 7.81 (br s, 3H, NH₂HCl), 5.71 (m, 1H), 5.16 (m, 2H, OCH₂CH=CH₂), 4.32 (m, 2H, OCH₂CH=CH₂), 2.40 (d, J = 7.00, 2H, H₉), 2.07 (m, 1H, H₁₃), 1.66 (m, 4H, H₁₁/H₁₂), 1.33 (m, 1H, H₁₀), 0.92 (m, 4H, H₁₁/H₁₂). ¹³C NMR (*d*₆-DMSO, 100 MHz), δ 174.77 (C1), 133.12 (OCH₂CH=CH₂), 117.78 (OCH₂CH=CH₂), 64.46 (OCH₂CH=CH₂), 44.01 (CH₂NH₂), 42.32 (C2), 35.12 (C4), 29.02 (C3, C5), 28.20 (C2, C6). Anal. Calc. for C₁₁H₁₉NO₂·HCl: C, 56.52; H, 8.62; N, 5.99. Found: C, 56.37; H, 8.54; N, 5.76%. FABMS (m/z): calc. for C₁₁H₂₀NO₂, 198.28 ([MH]⁺); found, 198.10.

Synthesis of ligands

L4. To a stirred suspension of DTPA-bis(anhydride) (1.79 g, 5 mmol) in dry DMF (15 mL) was added 2-hydroxyethyl-*trans*-4-(aminomethyl)cyclohexylcarboxylate hydrochloride (2.38 g, 10 mmol). The mixture was stirred at 70 °C for 4 h. The solvent was removed from the reaction mixture under reduced pressure, and the residue dissolved in methanol (10 mL). The solution was passed through a short column of silica gel (60 mesh) with methanol as an eluent. The residue obtained after removal of the solvent from the eluate was triturated with a mixture of acetone and diethyl ether (30 : 70 v/v, 150 mL). The solid product was

isolated by filtration, washed with acetone (3×30 mL), and dried *in vacuo* at 70°C for 8 h. Yield 3.93 g (87%). ^1H [d_6 -DMSO, 400 MHz], δ 8.25 (s, 2H, CH_2CONH), 4.17 (s, 2H, H2), 3.54 (m, 8H, $\text{OCH}_2\text{CH}_2\text{OH}$), 3.40 (m, 8H, H7, H5), 3.07 (m, 4H, H3/H4), 2.94 (m, 4H, H3/H4), 2.24 (m, 2H, H13), 2.08 (m, 4H, H9), 1.81 (m, 8H, H11/H12), 1.37 (m, 2H, H10), 1.08 (m, 8H, H11/H12). ^{13}C NMR (d_6 -DMSO, 100 MHz), δ 175.46 (C1/C8), 175.09 (C1/C8), 172.96 (C14), 172.26 (C6), 65.83 ($\text{OCH}_2\text{CH}_2\text{OH}$), 65.26 ($\text{OCH}_2\text{CH}_2\text{OH}$), 63.99 (C2), 59.25 (C7), 56.49 (C5), 54.83 (C3/C4), 54.54 (C3/C4), 44.84 (C13), 43.02 (C9), 42.76 (C10), 29.59 (C11), 28.52 (C12). Anal. Calc. for $\text{C}_{34}\text{H}_{57}\text{N}_5\text{O}_{14} \cdot 8\text{H}_2\text{O}$: C, 45.17; H, 8.14; N, 7.75. Found: C, 45.33; H, 7.86; N, 7.66%. FAB-MS (m/z): calc. for $\text{C}_{34}\text{H}_{58}\text{N}_5\text{O}_{14}$, 760.85 ($[\text{MH}]^+$), $\text{C}_{34}\text{H}_{57}\text{N}_5\text{NaO}_{14}$ 782.83 ($[\text{MNa}]^+$); found, 760.65 ($[\text{MH}]^+$), 782.60 ($[\text{MNa}]^+$).

L5. This compound was obtained essentially by following the same procedure as that for **L4** by replacing 2-hydroxyethyl-*trans*-4-(aminomethyl)cyclohexylcarboxylate hydrochloride with 2-methoxyethyl-*trans*-4-(aminomethyl)cyclohexylcarboxylate hydrochloride. Yield 3.87 g (83%). ^1H [d_6 -DMSO, 400 MHz], δ 8.31 (s, 2H, CH_2CONH), 4.14 (s, 2H, H2), 4.09 (m, 4H, $\text{OCH}_2\text{CH}_2\text{OCH}_3$), 3.56 (m, 4H, $\text{OCH}_2\text{CH}_2\text{OCH}_3$), 3.48 (m, 8H, H7, H5), 3.36 (m, 4H, H3/H4), 3.23 (s, 6H, $\text{OCH}_2\text{CH}_2\text{OCH}_3$), 3.08 (m, 4H, H3/H4), 2.93 (m, 4H, H9), 2.21 (m, 2H, H13), 1.76 (m, 8H, H11/H12), 1.37 (m, 2H, H10), 1.08 (m, 8H, H11/H12). ^{13}C [d_6 -DMSO, 100 MHz], δ 175.34 (C14), 172.88 (C1/C8), 172.05 (C1/C8), 170.09 (C6), 70.11 ($\text{OCH}_2\text{CH}_2\text{OCH}_3$), 63.20 ($\text{OCH}_2\text{CH}_2\text{OCH}_3$), 58.42 ($\text{OCH}_2\text{CH}_2\text{OCH}_3$), 56.45 (C2), 54.83 (C7), 54.55 (C5), 51.85 (C3/C4), 49.72 (C3/C4), 44.84 (C13), 42.66 (C9), 37.07 (C10), 29.53 (C11), 28.52 (C12). Anal. Calc. for $\text{C}_{36}\text{H}_{61}\text{N}_5\text{O}_{14} \cdot 8\text{H}_2\text{O}$: C, 46.39; H, 8.33; N, 7.51. Found: C, 46.22; H, 7.97; N, 7.83. FAB-MS (m/z): calc. for $\text{C}_{36}\text{H}_{62}\text{N}_5\text{O}_{14}$, 788.9 ($[\text{MH}]^+$); $\text{C}_{36}\text{H}_{61}\text{N}_5\text{NaO}_{14}$, 810.88 ($[\text{MNa}]^+$); found, 788.67 ($[\text{MH}]^+$), 810.61 ($[\text{MNa}]^+$).

L6. This compound was obtained essentially by following the same procedure as that for **L4** by replacing 2-hydroxyethyl-*trans*-4-(aminomethyl)cyclohexylcarboxylate hydrochloride with allyl-*trans*-4-(aminomethyl)cyclohexylcarboxylate hydrochloride. Yield 3.60 g (82%). ^1H NMR (d_6 -DMSO, 400 MHz), δ 8.28 (s, 2H, CH_2CONH), 5.89 (m, 2H, $\text{OCH}_2\text{CH}=\text{CH}_2$), 5.22 (m, 4H, $\text{OCH}_2\text{CH}=\text{CH}_2$), 4.52 (d, $J = 4.52$, 4H, $\text{OCH}_2\text{CH}=\text{CH}_2$), 4.15 (s, 2H, H2), 3.55 (m, 4H, H7), 3.48 (m, 4H, H5), 3.36 (m, 4H, H9), 3.08 (m, 4H, H3/H4), 2.94 (m, 4H, H3/H4), 2.25 (m, 2H, H13), 1.81 (m, 8H, H11/H12), 1.38 (m, 2H, H10), 1.12 (m, 8H, H11/H12). ^{13}C NMR (d_6 -DMSO, 100 MHz), δ 174.94 (C14), 172.93 (C1/C8), 172.13 (C1/C8), 170.24 (C6), 133.14 ($\text{OCH}_2\text{CH}=\text{CH}_2$), 117.75 ($\text{OCH}_2\text{CH}=\text{CH}_2$), 64.41 ($\text{OCH}_2\text{CH}=\text{CH}_2$), 56.46 (C2), 54.81 (C7), 54.55 (C5), 53.05 (C3/C4), 52.27 (C3/C4), 44.85 (C13), 42.70 (C9), 37.09 (C10), 29.58 (C11), 28.55 (C12). Anal. Calc. for $\text{C}_{36}\text{H}_{57}\text{N}_5\text{O}_{12} \cdot 7\text{H}_2\text{O}$: C, 49.25; H, 8.15; N, 7.98. Found: C, 49.13; H, 7.80; N, 8.17. FAB-MS (m/z): calc. for $\text{C}_{36}\text{H}_{58}\text{N}_5\text{O}_{12}$, 752.41 ($[\text{MH}]^+$); $\text{C}_{36}\text{H}_{57}\text{N}_5\text{NaO}_{12}$, 774.39 ($[\text{MNa}]^+$); found, 752.55 ($[\text{MH}]^+$), 774.50 ($[\text{MNa}]^+$).

Synthesis of complexes

[Gd(L4)H₂O]. To a solution of **L4** (1.81 g, 2 mmol) in dry pyridine (10 mL) was added gadolinium(III) acetate tetrahydrate (0.81 g, 2 mmol). The suspension was stirred for 6 h at 70°C

during which time a pale yellow solution resulted. Solvent from the reaction mixture was stripped off and the residue was taken in ethanol (40 mL). The resulting solution was refluxed for 2 h. The reaction mixture was cooled and passed through a Celite column to remove any solid impurities. The solvent was removed and the residue taken up in ethanol (5 mL). The title complex was precipitated as a white solid by adding the ethanolic solution dropwise into acetone at 0°C . The product was isolated by filtration, washed thoroughly with acetone, dried *in vacuo* at 80°C for 8 h. Yield 1.89 g (88%). Anal. Calc. for $\text{C}_{34}\text{H}_{56}\text{GdN}_5\text{O}_{15} \cdot \text{H}_2\text{O}$: C, 37.94; H, 6.74; N, 6.51. Found: C, 37.92; H, 6.48; N, 6.88. FABMS (m/z): calc. for $\text{C}_{34}\text{H}_{57}\text{GdN}_5\text{O}_{15}$, 933.09 ($[\text{MH}]^+$), $\text{C}_{34}\text{H}_{55}\text{GdN}_5\text{O}_{14}$, 915.08 ($\text{MH} - (\text{H}_2\text{O})^+$); found, 932.77 ($[\text{MH}]^+$), 914.84 ($\text{MH} - (\text{H}_2\text{O})^+$).

[Gd(L5)H₂O]. This compound was obtained essentially by following the same procedure as that for **[Gd(L4)H₂O]** by replacing **L4** with **L5**. Yield 1.98 g (90%). Anal. Calc. for $\text{C}_{36}\text{H}_{60}\text{GdN}_5\text{O}_{15} \cdot 8\text{H}_2\text{O}$: C, 39.16; H, 6.94; N, 6.34. Found: C, 39.02; H, 6.70; N, 6.65. FABMS (m/z): calc. for $\text{C}_{36}\text{H}_{59}\text{GdN}_5\text{O}_{14}$, 943.13 ($\text{MH} - (\text{H}_2\text{O})^+$); found, 942.78 ($\text{MH} - (\text{H}_2\text{O})^+$).

[Gd(L6)H₂O]. This compound was obtained essentially by following the same procedure as that for **[Gd(L4)H₂O]** by replacing **L4** with **L6**. Yield 1.80 g (87%). Anal. Calc. for $\text{C}_{36}\text{H}_{56}\text{GdN}_5\text{O}_{13} \cdot 6\text{H}_2\text{O}$: C, 41.89; H, 6.64; N, 6.78. Found: C, 42.09; H, 6.47; N, 6.97. FABMS (m/z): calc. for $\text{C}_{36}\text{H}_{55}\text{GdN}_5\text{O}_{12}$, 907.1 ($\text{MH} - (\text{H}_2\text{O})^+$); found, 906.78 ($\text{MH} - (\text{H}_2\text{O})^+$).

Relaxivity

T_1 measurements were carried out using an inversion recovery method with a variable inversion time (TI) at 1.5 T (64 MHz). The magnetic resonance (MR) images were acquired at 35 different TI values ranging from 50 to 1750 ms. T_1 relaxation times were obtained from the non-linear least square fit of the signal intensity measured at each TI value. For T_2 measurements the CPMG (Carr–Purcell–Meiboom–Gill) pulse sequence was adapted for multiple spin–echo measurements. Thirty four images were acquired with 34 different echo time (TE) values ranging from 10 to 1900 ms. T_2 relaxation times were obtained from the non-linear least squares fit of the mean pixel values for the multiple spin–echo measurements at each echo time. Relaxivities (R_1 and R_2) were then calculated as an inverse of relaxation time per mM. The determined relaxation times (T_1 and T_2) and relaxivities (R_1 and R_2) are finally image-processed to give the relaxation time map and relaxivity map, respectively.

In vitro determination of cell toxicity

14D Chick cornea stroma primary cells (p1) were used. These cell lines were obtained from Department of Biology, College of Natural Sciences, Kyungpook National University. The cells were grown in 100 cm^2 plastic culture dishes (Corning culture dish) in 10 mL of medium at 37°C and in a humidified 5% CO_2 atmosphere. Cells were maintained in F-12-medium (Gibco) supplemented with heat-inactivated 10% FCS, 1% chicken serum, 5 mg mL^{-1} insulin, 10 ng mL^{-1} human recombinant EGF, 100 IU mL^{-1} penicillin, 100 mg mL^{-1} streptomycin and 200 mg mL^{-1} gentamicin (all purchased from Gibco). The medium was replaced every two days, and cells were split into 96-well plate (6×10^4 cells

well⁻¹ (200 μ L)). Various concentrations (0.5–10 mM) of Gd complexes were added into the culture serum free media and incubated for 24 h. Cell viability/toxicity assessment was performed by using Cell Counting Kit (CCK-8), which was purchased from Dojindo Laboratory, Japan. 10 μ L of CCK-8 solution was directly added to each well and the plate was incubated at 37 $^{\circ}$ C for 3 h. The O.D. was read at 490 nm using an ELISA (Molecular Device, USA Bio-rad 550 Reader) to determine the cell viability/toxicity in each well.

Animal tumor model

The mice were maintained according to protocols approved by the Institutional Animal Care and Use Committee, KNU. 18-Week old H-ras12V transgenic mouse bearing hepatocellular carcinoma (35 g) was included in this study. Animals were anaesthetized with an intramuscular injection of 50 μ L xylazine (Rompun: 20 mg mL⁻¹) and 10 μ L ketamine (Ketalar: 50 mg mL⁻¹). [Gd(L2)(H₂O)] was injected into a tail vein at a dosage of 1.43 mmol kg⁻¹.

MR Imaging

MR images of anaesthetized mice were obtained pre- and post-[Gd(L2)(H₂O)] injection during 75 min with a 1.5 T scanner (GE Signa Advantage, GE Medical system, USA) and extremity coil. The animals were placed in the magnet in a supine position with the heads firmly fixed. After each measurement the animals were revived from anaesthesia, and placed in their cages with free access to food and water. During MRI measurements, the animals were maintained at approximately 37.0 $^{\circ}$ C using a warm water blanket. The imaging parameters for FSPGR (fast spoiled gradient echo) were as follows: flip angle of 60 $^{\circ}$, 12 \times 12 mm field of view, 256 \times 128 matrix size, 22 axial slices, 2 mm slice thickness, slice gap of 0 mm, repetition time (TR) = 70 ms, echo time (TE) = 3 ms and number of acquisitions (NEX) = 2.

Image analysis

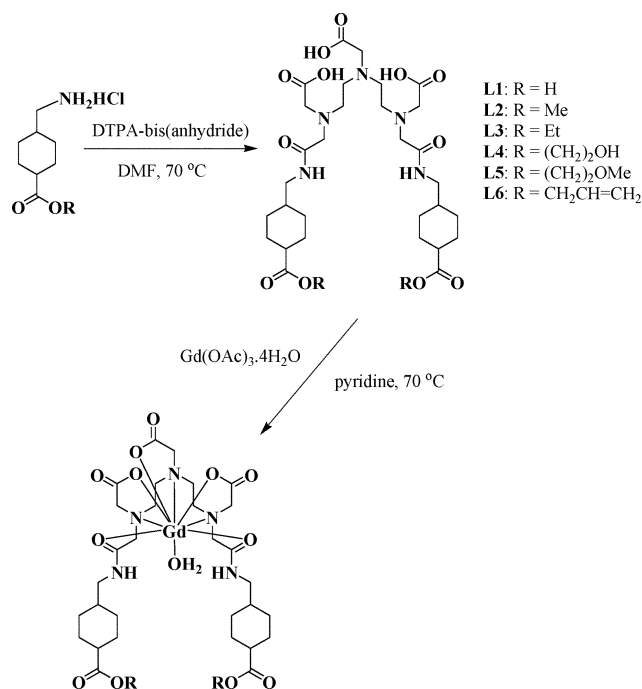
The anatomical locations with enhanced contrast were identified with respect to hepatocellular carcinoma of the liver on post-contrast MR images. For quantitative measurement, signal intensities in specific regions of interest (ROI) of 20–40 mm³ were measured using Advantage Window software (GE Medical, USA). Multiple areas were sampled throughout the tumor and averaged to give a mean SI value for that tissue. The percentage of contrast enhancement in the signal from the tumor was calculated using eqn (1), where SI is the signal intensity.

$$\text{Enhancement (\%)} = 100(\text{SI}_{\text{post}} - \text{SI}_{\text{pre}})/\text{SI}_{\text{pre}} \quad (1)$$

Results and discussion

Synthesis

Scheme 1 shows the preparative method leading to the formation of DTPA-bis(amides) functionalized by *trans*-4-(aminomethyl)-cyclohexanecarboxylates (L) and their Gd(III) complexes of the type [Gd(L)(H₂O)] \cdot *n*H₂O (L = L1–L6). The synthesis initially involves esterification of *trans*-4-(aminomethyl)cyclo-



Scheme 1

hexanecarboxylic acid (tranexamic acid) by treating it with a slight excess of thionyl chloride in the corresponding alcohol as a solvent. Simple condensation of DTPA-bis(anhydride) with two equivalents of acid/esters in DMF resulted in corresponding DTPA-bis(amides) (L1–L6) in almost quantitative yields. All these ligands were characterized by analytical and spectroscopic techniques (¹H and ¹³C NMR and FAB-mass). IR spectroscopy is also informative in that the presence of carbonyl groups in each ligand can be confirmed by a pair of intense carbonyl stretching bands assignable to the amide carbonyl (NHC=O) and carboxylic carbonyl (C=O) groups in the range 1602–1672 cm⁻¹.¹⁷

These ligands form Gd(III) complexes of the type [Gd(L)(H₂O)] \cdot *n*H₂O (L = L1–L6) by simple complexation with an equimolar amount of gadolinium acetate in pyridine as illustrated in Scheme 1. All complexes were isolated as a white solid by precipitating in cold acetone from the reaction mixture. The complexes are highly hygroscopic, and isolated as hydrated solids.

Protonation constants and stability constants

The protonation constants (*K*_i^H) of the ligands and the stability constants of the metal complexes are defined in eqn (2) and (3), respectively, where H_{*i*}L (*i* = 1, 2, ...) is the protonated ligand, L totally deprotonated free ligand, M unhydrolyzed aqua metal ion, and ML the non-protonated and unhydrolyzed complex.

$$K_i^H = [\text{H}_i\text{L}]/[\text{H}_{i-1}\text{L}][\text{H}^+] \quad (2)$$

$$K_{\text{ML(therm)}} = [\text{ML}]/[\text{M}][\text{L}] \quad (3)$$

The protonation constants of L1–L6 and the stability constants of their Gd(III), Ca(II), Zn(II) and Cu(II) complexes were determined by potentiometric titration, and relevant data are collected in Table 1 along with those for DTPA and DTPA-BMA for comparative purposes. It is known that for the DTPA-bis(amide)

Table 1 Protonation constants ($\log K_i^H$) of **L1–L6**, stability (K_{ML}), selectivity constants (K_{sel}) and conditional stability constants (K'_{sel}) of Gd-complexes of **L1–L6** ($I = 0.10 \text{ mol dm}^{-3}$), and pM^a values of the complexes of Gd(III), Zn(II), Ca(II) and Cu(II) at pH 7.4

| Equilibrium | $\log K$ (25 °C, $\mu = 0.10 \text{ M (KCl)}$) | | | | | | DTPA-BMA ^b | DTPA ^c |
|--|---|-----------|-----------|-----------|-----------|-----------|-----------------------|-------------------|
| | L1 | L2 | L3 | L4 | L5 | L6 | | |
| [HL]/[L][H] | 11.43 | 9.74 | 9.77 | 9.94 | 9.95 | 9.81 | 9.37 | 10.49 |
| [H ₂ L]/[HL][H] | 10.03 | 5.02 | 5.10 | 5.15 | 5.18 | 4.81 | 4.38 | 8.60 |
| [H ₃ L]/[H ₂ L][H] | 5.72 | 3.21 | 3.31 | 3.72 | 3.79 | 3.67 | 3.31 | 4.28 |
| [H ₃ L]/[H ₄ L][H] | 4.47 | — | — | — | — | — | — | 2.64 |
| $\sum pK_a$ | 29.60 | 17.97 | 18.18 | 18.81 | 18.92 | 18.29 | 17.06 | 26.01 |
| [GdL]/[Gd][L] | 22.38 | 20.42 | 20.55 | 21.10 | 20.80 | 20.99 | 16.85 | 22.46 |
| { $\log K_{GdL}$ (pH 7.4)} | 15.71 | 18.08 | 18.18 | 18.56 | 18.25 | 18.58 | 14.84 | 18.14 |
| [CaL]/[Ca][L] | 14.81 | 7.50 | 7.36 | 7.85 | 7.86 | 7.17 | 7.17 | 10.75 |
| { $\log K_{CaL}$ (pH 7.4)} | 8.14 | 5.16 | 4.99 | 5.31 | 5.31 | 4.76 | 5.11 | 6.43 |
| [ZnL]/[Zn][L] | 16.65 | 12.26 | 12.32 | 11.78 | 11.80 | 11.03 | 12.04 | 18.70 |
| { $\log K_{ZnL}$ (pH 7.4)} | 9.98 | 9.91 | 9.95 | 9.24 | 9.25 | 8.62 | 10.02 | 14.38 |
| [CuL]/[Cu][L] | 11.87 | 13.04 | 12.74 | 12.46 | 12.23 | 11.52 | 13.03 | 21.38 |
| { $\log K_{CuL}$ (pH 7.4)} | 5.20 | 10.70 | 10.37 | 9.92 | 9.68 | 9.11 | 11.06 | 17.06 |
| $\log K_{sel}$ (Gd/Ca) | 14.19 | 12.92 | 13.19 | 13.25 | 12.94 | 13.82 | 9.68 | 11.71 |
| $\log K_{sel}$ (Gd/Zn) | 5.73 | 8.16 | 8.23 | 9.32 | 9.00 | 9.96 | 4.81 | 3.76 |
| $\log K_{sel}$ (Gd/Cu) | 12.14 | 7.38 | 7.81 | 8.64 | 8.57 | 9.47 | 3.82 | 1.08 |
| $\log K'_{sel}$ | 10.03 | 12.41 | 12.51 | 13.58 | 13.27 | 14.23 | 9.03 | 7.04 |
| pGd | 14.71 | 17.08 | 17.18 | 17.56 | 17.25 | 17.58 | 13.88 | 17.14 |
| pCa | 7.14 | 4.16 | 3.99 | 4.31 | 4.31 | 3.76 | 4.19 | 5.45 |
| pZn | 8.98 | 8.92 | 8.95 | 8.24 | 8.25 | 7.61 | 9.06 | 13.39 |
| pCu | 4.20 | 9.70 | 9.37 | 8.92 | 8.68 | 8.11 | 10.05 | 16.06 |

^a $pM = -\log[M^{n+}]_{free}$ at pH 7.4; $[M^{n+}]_{total} = 1 \mu\text{mol dm}^{-3}$; $[L]_{total} = 1.1 \mu\text{mol dm}^{-3}$. ^b Data obtained from ref. 21. ^c Data obtained from ref. 31.

ligands the first protonation constant (K_1^H) takes place at the central nitrogen atom, while the second (K_2^H) and the third (K_3^H) at the terminal amine nitrogen atoms.¹²

Table 1 shows that all ligands (**L1–L6**) exhibit higher protonation constants ($\log K_i^H$) and $\sum pK_a$ values than DTPA-BMA. It is probable that the presence of carboxylic acid (**L1**) or esters (**L2–L6**) in the amide side-arms seems to render the protonation of the amine nitrogen(s) facile by some co-operative interaction to exhibit higher protonation constants. When the comparison is made among the present series, **L1** shows the highest values and even higher values than the parent DTPA. In general, substitution of the acetate groups on the terminal amine nitrogen atoms of DTPA reduces its basicity, as reflected in the lower $\log K_i^H$ and $\sum pK_a$ values of corresponding DTPA-bis-amide ligands. High basicity of **L1–L6** will surely lead to high thermodynamic stability of their metal complexes.

Table 1 shows the thermodynamic stability constants for the complexes of Ca(II), Zn(II), and Cu(II) complexes. A direct potentiometric method can not be applied for the measurement of the stability constants of $[Gd(L)(H_2O)]$ (**L** = **L1–L6**) since they are formed at low pH. Instead, they were determined by employing the method of ligand–ligand competition potentiometric titration between EDTA and **L1–L6** for Gd(III) ion.^{22–24} Thermodynamic stability of Gd(III) complexes measures the tendency of dissociation of the complexes in solution to generate free Gd(III) ion, which shows acute cytotoxicity in the physiological system. The table shows quite expectedly that high basicity of **L1–L6** leads to high

thermodynamic stability of their metal complexes as compared with that of the corresponding metal complexes of DTPA-BMA, with **L1** exhibiting the highest thermodynamic stability for the same reason described above.

However, the thermodynamic stability constant alone is insufficient to account for the stability of the complexes under the physiological condition.^{21,25} The conditional stability constant or more frequently the pM value is apt to describe the stability of complexes under physiologically relevant conditions.²⁶ The pM value reflects the influence of ligand basicity and protonation of the complex. Thus, the larger the pM value, the higher the affinity of the ligand for the metal ion under the given condition.²⁷ Table 1 shows that **L1–L6** exhibit higher pM values with Gd(III) than with Ca(II), Zn(II) or Cu(II); the indication is that the Gd(III) complexes of **L1–L6** are stable enough to avoid any interference by other endogenous metal ions. In addition to the pM value, the conditional stability constant (K'_{sel}) has also to be taken into consideration under the physiological condition. This is because a Gd(III) complex injected as an MRI CA into the physiological system through the blood pool competes not only with endogenous metal ions such as Ca(II), Zn(II) and Cu(II) but also with protons at the physiological pH.²⁶ The conditional stability constant (K'_{sel}) can be calculated by considering all equilibria present at physiological pH.²¹ The K'_{sel} have been shown to correlate with the experimental LD_{50} value.²⁸ Table 1 demonstrates that **L1–L6** reveal higher $\log K'_{sel}$ values than DTPA-BMA and DTPA suggesting that their Gd(III) complexes should exhibit little cytotoxicity.

Relaxivity

Fig. 1 shows the relaxation time (T_1) and relaxivity (R_1) maps on $[\text{Gd}(\text{L})(\text{H}_2\text{O})]$ ($\text{L} = \text{L1-L6}$), Omniscan[®], and pure water. The phantom images were obtained with 1 mM solution of complexes and with the same concentration of Omniscan[®] for comparative purposes. Table 2 summarizes the relaxation times (T_1 and T_2) and relaxivities (R_1 and R_2) for the Gd-complexes, Omniscan[®], and pure water.

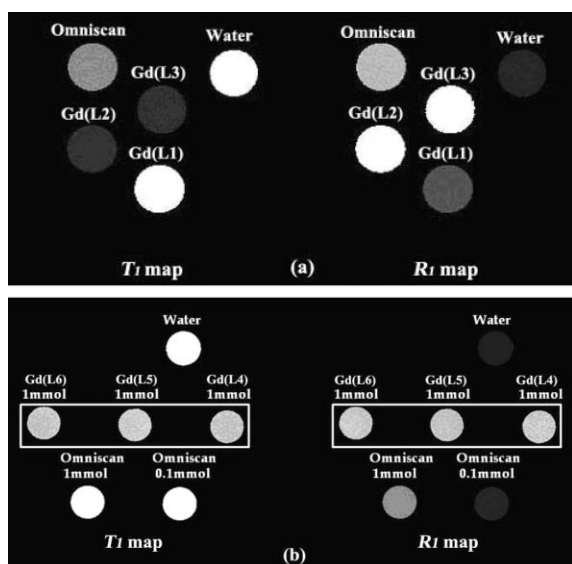


Fig. 1 T_1 and R_1 maps on (a) $[\text{Gd}(\text{L})(\text{H}_2\text{O})]$ ($\text{L} = \text{L1-L3}$), Omniscan[®], and pure water; (b) $[\text{Gd}(\text{L})(\text{H}_2\text{O})]$ ($\text{L} = \text{L4-L6}$), Omniscan[®], and pure water.

The most significant feature of Table 2 is that all complexes except for $[\text{Gd}(\text{L1})(\text{H}_2\text{O})]$ exhibit significantly high R_1 values. Increased relaxivities with **L2-L6** may be explained not only in terms of increased molecular weight as compared with DTPA-BMA but also of some co-operative interaction between the coordinated water and the carboxylic groups on the cyclohexyl moiety. For instance, the rate of water exchange in **L2** and **L3** seems to be enhanced by the presence of hydrophobic alkyl esters. On the other hand, other esters (**L4-L6**) seem to retard the water-exchange rate for some unknown reasons. The lowest relaxivity value found with **L1** may be attributed to the interaction of the carboxylic acid with coordinated water through hydrogen bonding, thereby lowering the exchange rate.²⁰

In vivo MRI test

The *in vivo* MRI test was performed with $[\text{Gd}(\text{L2})(\text{H}_2\text{O})]$. The solution of this complex was injected into the H-*ras* transgenic mice bearing hepatic tumors, and the contrast enhancement of the MR images evaluated using Omniscan[®] as the control. Fig. 2 shows the T_1 -weighted images of hepatocellular carcinoma (HCC) before and after injection. The signal intensities (SI) after injection are enhanced when compared with the SI obtained in the absence of the contrast agent. The MR images of the tumor become brighter after injection, and the demarcation from the surrounding tissues becomes clear as a result of the contrast enhancement. The enhanced contrast of the kidney was observed, thus confirming the renal excretion of the contrast agent.

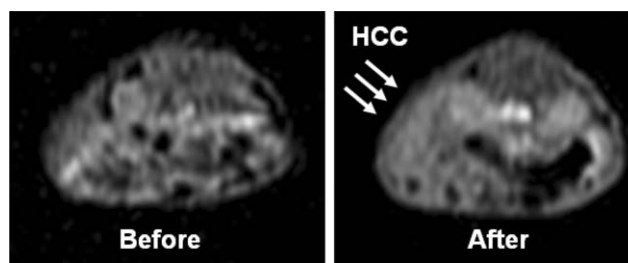


Fig. 2 The T_1 -weighted images of the tumor bearing H-*ras* transgenic mice: (a) pre-injection image; (b) 20 min after injection with $[\text{Gd}(\text{L2})(\text{H}_2\text{O})]$ at the dosage of $1.43 \text{ mmol kg}^{-1}$.

Fig. 3 shows the MR signal intensity enhancements (IEs) as a function of time after injection of $[\text{Gd}(\text{L2})(\text{H}_2\text{O})]$ and Omniscan[®] for comparative purposes. The most significant feature is that $[\text{Gd}(\text{L2})(\text{H}_2\text{O})]$ exhibits a much higher contrast enhancement than Omniscan[®] throughout the measurement ($\sim 80 \text{ min}$) at the same Gd-concentration. It is worth noting, for example, that the IE with $[\text{Gd}(\text{L2})(\text{H}_2\text{O})]$ becomes nearly 12 times as high as that with Omniscan[®] in 20 min after injection. Furthermore, such high IE with $[\text{Gd}(\text{L2})(\text{H}_2\text{O})]$ remains almost steady during the measurement, thus making it possible to acquire a number of MR images.

In vitro toxicity study

An additional observation with $[\text{Gd}(\text{L2})(\text{H}_2\text{O})]$ is that all mice recovered spontaneously from anaesthesia after the MRI measurements, thus providing motivation for toxicity studies on this complex. Fig. 4 shows the results of the MTT assay (MTT = 3-(4,5-dimethylthiazol-2-yl)-2,5-diphenyltetrazolium bromide) performed to evaluate the cytotoxic effects of $[\text{Gd}(\text{L})(\text{H}_2\text{O})]$

Table 2 T_1 , R_1 , T_2 and R_2 values for the Gd complexes, Omniscan[®], and pure water^a

| Sample | T_1/ms | $R_1/\text{mM}^{-1} \text{ s}^{-1}$ | T_2/ms | $R_2/\text{mM}^{-1} \text{ s}^{-1}$ |
|--|-------------------|-------------------------------------|--------------------|-------------------------------------|
| $[\text{Gd}(\text{L1})(\text{H}_2\text{O})]$ | 477.5 ± 9.94 | 2.1 ± 0.05 | 550.9 ± 22.05 | 1.8 ± 0.07 |
| $[\text{Gd}(\text{L2})(\text{H}_2\text{O})]$ | 79.05 ± 3.99 | 12.7 ± 0.66 | 113.9 ± 14.39 | 8.7 ± 0.88 |
| $[\text{Gd}(\text{L3})(\text{H}_2\text{O})]$ | 78.28 ± 4.68 | 12.9 ± 0.84 | 131.5 ± 0.002 | 7.2 ± 1.9 |
| $[\text{Gd}(\text{L4})(\text{H}_2\text{O})]$ | 123.29 ± 4.47 | 8.1 ± 0.28 | 232.54 ± 13.05 | 4.3 ± 0.24 |
| $[\text{Gd}(\text{L5})(\text{H}_2\text{O})]$ | 126.98 ± 4.23 | 7.9 ± 0.25 | 227.55 ± 13.53 | 4.4 ± 0.26 |
| $[\text{Gd}(\text{L6})(\text{H}_2\text{O})]$ | 123.67 ± 3.61 | 8.1 ± 0.23 | 240.80 ± 12.44 | 4.2 ± 0.21 |
| Omniscan [®] | 209.8 ± 5.82 | 4.9 ± 0.14 | 290.8 ± 21.02 | 3.4 ± 0.25 |
| Water | 842.5 ± 46.38 | 1.1 ± 0.06 | 1220 ± 167.20 | 0.82 ± 0.12 |

^a Each value is presented as a mean value (\pm SD).

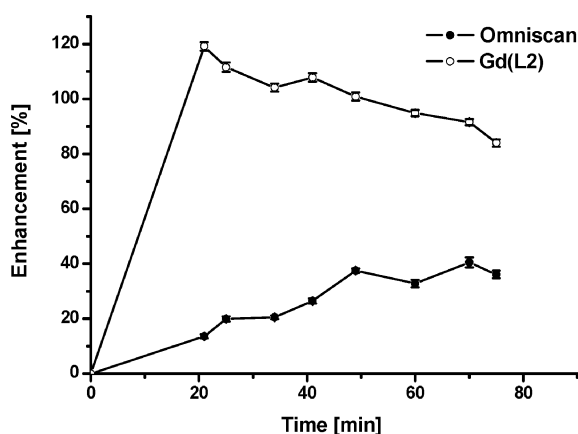


Fig. 3 Time dependent MR signal intensity enhancement of the tumor in a mouse after injection with [Gd(L2)(H₂O)] and Omniscan® at the dosage of 1.43 mmol kg⁻¹.

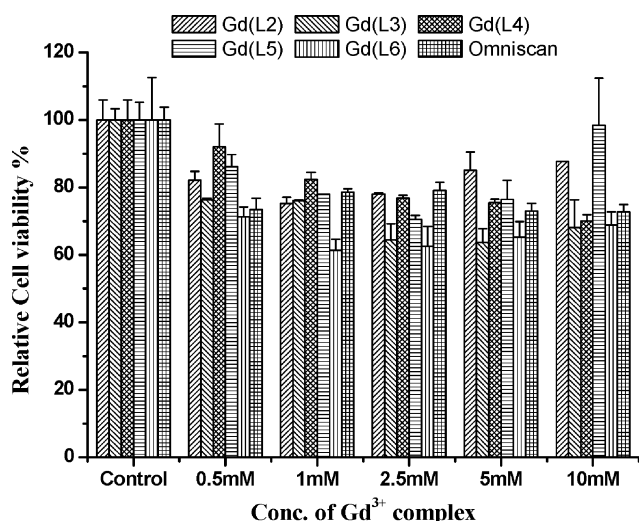


Fig. 4 Relative cell viability (%) of the 14D Chick cornea stroma primary cells obtained by [Gd(L)(H₂O)] and Omniscan®. The standard deviations (\pm SD) were obtained on a triplicate analysis ($n = 3$).

(L = L2–L6) using 14D Chick cornea stroma primary cells.^{29,30} Each set of experiments employ the complexes with the concentration range of 0.5–10 mM in a serum-free medium, along with the control experiment with cells in the absence of any contrast agent. Separate experiments were also performed with Omniscan® for comparative purposes.

Fig. 4 demonstrates that the cell proliferation and the viability are not affected when incubated for 24 h. No obvious change is observed when a comparison is made between the cells of the cell viability assessment with the contrast agents and those for the control. These observations indicate that [Gd(L)(H₂O)] (L = L2–L6) have very low cytotoxicity in the concentration range required for obtaining intensity enhancement in the MR images.

Conclusions

The synthesis and characterization of DTPA-bis(amide) conjugates of tranexamic acid (L1), its esters (L2–L6), and their Gd(III) complexes of the type [Gd(L)(H₂O)]·*n*H₂O (L = L1–L6) are

described. The potentiality of Gd-complexes as practical MRI CAs was investigated by measuring not only their R_1 relaxivity but also other relevant physicochemical properties and cytotoxicity. All Gd-complexes except for the case of L1 exhibit much higher R_1 relaxivity than Omniscan®; the highest R_1 reaches up to 2.6 times that for Omniscan®. Such high relaxivity is reflected in the intensity enhancement of the *in vivo* MRI study on H-*ras* transgenic mice bearing hepatic tumors when employing these new complexes as MRI CAs. Thermodynamic stability constants, conditional stability constants, and the pM values also demonstrate higher stability of these complexes under physiological conditions. The MTT assay performed on these complexes reveals cytotoxicity as low as that for Omniscan® in the concentration range required to obtain intensity enhancement in the *in vivo* MRI study.

Acknowledgements

This work was supported by a grant from The Advanced Medical Technology Cluster for Diagnosis and Prediction at KNU from MOCIE, ROK. Spectral measurements were performed by the KBSI.

Notes and references

- 1 P. Caravan, *Chem. Soc. Rev.*, 2006, **35**, 512.
- 2 K. N. Raymond and V. C. Pierre, *Bioconjugate Chem.*, 2005, **16**, 3.
- 3 *The Chemistry of Contrast Agents in Medical Magnetic Resonance Imaging*, ed. É. Tóth and A. E. Merbach, Wiley, Chichester, 2001.
- 4 P. Caravan, J. J. Ellison, T. J. McMurphy and R. B. Lauffer, *Chem. Rev.*, 1999, **99**, 2293.
- 5 S. W. A. Bligh, A. H. M. S. Chowdhury, M. McPartlin, I. J. Scowen and R. A. Bulman, *Polyhedron*, 1995, **14**, 567.
- 6 H. Lammers, F. Maton, D. Pubanz, M. W. Van Laren, H. Van Bakkum, A. E. Merbach, R. N. Muller and J. A. Peters, *Inorg. Chem.*, 1997, **36**, 2527.
- 7 S. Aime, F. Benetollo, G. Bombieri, S. Colla, M. Fasano and S. Paoletti, *Inorg. Chim. Acta*, 1997, **254**, 63.
- 8 X. Zhao, R. Zhuo, Z. Lu and W. Liu, *Polyhedron*, 1997, **16**, 2755.
- 9 H. Lammers, A. M. van der Heijden, H. van Bakkum, C. F. G. C. Geraldes and J. A. Peters, *Inorg. Chim. Acta*, 1998, **268**, 249.
- 10 S. W. A. Bligh, A. H. M. S. Chowdhury, D. Kennedy, C. Luchinat and G. Parigi, *Reson. Med.*, 1999, **41**, 767.
- 11 Y.-M. Wang, Y.-J. Wang, R.-S. Sheu, G.-C. Liu, W.-C. Liu and J.-H. Liao, *Polyhedron*, 1999, **18**, 1147.
- 12 C. F. G. C. Geraldes, A. M. Urbano, M. C. Alpoim, A. D. Sherry, K.-T. Kuan, R. Rajagopalan, F. Maton and R. N. Muller, *Magn. Reson. Imaging*, 1995, **13**, 401.
- 13 S. Dutta, S.-K. Kim, D. B. Patel, T.-J. Kim and Y. Chang, *Polyhedron*, 2007, **26**, 3799.
- 14 C. M. Savahn, F. Merenyi, L. Karlson, L. Widlund and M. Gralls, *J. Med. Chem.*, 1986, **29**, 448.
- 15 Y. Katsuta, Y. Yoshida, E. Kawai, M. Suetsugu, Y. Kohno, S. Inomata and K. Kitamura, *J. Dermatol. Sci.*, 2005, **40**, 218.
- 16 J. P. Guo, B. P. Liu, X. C. Lv, Z. C. Tan, B. Tong, Q. Shi and D. F. Wang, *J. Chem. Eng. Data*, 2007, **52**, 1678.
- 17 W. C. Eckelman, S. M. Karesh and R. C. Reba, *J. Pharm. Sci.*, 1975, **64**, 704.
- 18 S. Dutta, S.-K. Kim, E. J. Lee, T.-J. Kim, D.-S. Kang, Y. Chang, S. O. Kang and W.-S. Han, *Bull. Korean Chem. Soc.*, 2006, **27**, 1038.
- 19 P. Gans, A. Sabatini and A. Vacca, *Talanta*, 1996, **43**, 1739.
- 20 S. Laurent, T. N. Parac-Vogt, K. Kimpe, C. Thirifays, K. Binnemans, R. N. Muller and L. Vander Elst, *Eur. J. Inorg. Chem.*, 2007, **14**, 2061.
- 21 W. P. Cacheris, S. C. Quay and S. M. Rocklage, *Magn. Reson. Imaging*, 1990, **8**, 467.
- 22 W. R. Harris and A. E. Martell, *Inorg. Chem.*, 1976, **15**, 713.
- 23 Y. Li, A. E. Martell, R. D. Hancock, J. H. Reibenspies, C. J. Anderson and M. J. Welch, *Inorg. Chem.*, 1996, **35**, 404.

-
- 24 C. H. Taliaferro, R. J. Motekaitis and A. E. Martell, *Inorg. Chem.*, 1984, **23**, 1188.
- 25 K. Kumar, M. F. Tweedle, M. F. Malley and J. Z. Gougoutas, *Inorg. Chem.*, 1995, **34**, 6472.
- 26 S. Laus, R. Ruloff, E. Tóth and A. E. Merbach, *Chem.–Eur. J.*, 2003, **9**, 3555.
- 27 C. J. Bannochie and A. E. Martell, *Inorg. Chem.*, 1991, **30**, 1385.
- 28 M. F. Tweedle, J. J. Hahan, K. Kumar, S. Mantha and C. A. Chang, *Magn. Reson. Imaging*, 1991, **9**, 409.
- 29 C. Zou and Z. Shen, *J. Pharmacol. Toxicol. Methods*, 2007, **56**, 58.
- 30 M.-I. Huh, Y.-M. Lee, S.-K. Seo, B.-S. Kang, Y. Chang, Y.-S. Lee, M. E. Fini, S.-S. Kang and J.-C. Jung, *J. Cell. Biochem.*, 2007, **101**, 1222.
- 31 A. E. Martell and R. M. Smith, *Critical Stability Constants*, Plenum, New York, 1974, vol. 1.